Applied Catalysis A: General 497 (2015) 153–159

Contents lists available at ScienceDirect

Applied Catalysis A: General

journal homepage: www.elsevier.com/locate/apcata

Activity enhancement of Nafion resin: Vapor-phase carbonylation of dimethoxymethane over Nafion-silica composite

Shiping Liu[a,b], Wenliang Zhu[a], Lei Shi[a], Hongchao Liu[a], Yong Liu[a], Youming Ni[a], Lina Li[a,b], Hui Zhou[a,b], Shutao Xu[a], Yanli He[a], Zhongmin Liu[a,*]

[a] National Engineering Laboratory for Methanol to Olefins, Dalian National Laboratory for Clean Energy, Dalian Institute of Chemical Physics, Chinese Academy of Sciences, Dalian 116023, PR China
[b] University of Chinese Academy of Sciences, Beijing 100049, PR China

ARTICLE INFO

Article history:
Received 23 December 2014
Received in revised form 7 March 2015
Accepted 10 March 2015
Available online 18 March 2015

Keywords:
Dimethoxymethane
Carbonylation
Ethylene glycol
Methyl methoxy acetate
Nafion-silica composite

ABSTRACT

A kind of composite materials consisting of nano-sized Nafion resin homogeneously dispersed in a high-surface silica matrix was prepared by sol–gel method and used as catalysts in the vapor-phase carbonylation reaction of dimethoxymethane for production of methylmethoxy acetate. These composite catalysts showed much higher catalytic activity in comparison with the original pure Nafion resin catalyst. The remarkable improvement of catalytic performance was due to the increased accessibility of acid sites of Nafion resin in the composite catalysts. The contents of Nafion-H resin and silica precursors were found to have a great influence on the structure of the composite, resulting in different catalytic activity during DMM carbonylation reactions. Furthermore, the comparison of the composite catalysts with high-silica H-Y and H-Beta zeolite catalysts demonstrated that the excellent catalytic performance is closely related to the higher acid strength and larger pores of Nafion-silica composite materials.

1. Introduction

Ethylene glycol (EG), an important automotive antifreeze and an intermediate for polyester resins and fibers [1], has a worldwide capacity of about 23 million tons per year, and the demand for this chemical is expected to grow in the future [2]. Presently, EG is mainly produced through the hydration of ethylene oxide synthesized by the partial oxidation of petroleum-derived ethylene. The depleting of limited oil reservoirs has made it necessary and pressing to consider alternative starting materials for EG synthesis. Syngas, which is a mixture of CO and H_2 and can be readily generated from non-oil-based feedstocks such as the relatively abundant coal, natural gas, and renewable biomass, is a potential candidate for EG synthesis. One of attractive routes using syngas as the staring material is the carbonylation of formaldehyde catalyzed by acids to glycolic acid followed by esterification and hydrogenation [3,4]. However, acid-catalyzed carbonylation of formaldehyde, the key step during EG synthesis, has been exclusively conducted with strong liquid mineral acids, such as H_2SO_4 and HF, in liquid phase under high pressure [3,5]. One major concern about this process is the use of highly corrosive acids as homogenous catalysts, resulting in server environmental and safety problems. In the previous studies, more environmentally friendly solid acids, including acidic resins [6], acidic zeolites [7], and heteropolyacids [8], have been explored to replace strong homogenous catalysts to solve the corrosion problem, but the catalytic performance of these heterogeneous catalysts is inferior to that of homogeneous systems. On the other hand, the solubility of CO in most solvents is poor [9] and high pressure is required to promote CO concentration in liquid phase. Up to now, the development of a highly selective and environmentally benign process for the carbonylation of formaldehyde is still a challenge.

Recently, the carbonylation of dimethoxymethane (DMM), a derivative of formaldehyde, was reported with acidic zeolite catalysts in gas phase [10]. Cliek et al. reported that the selectivity of aimed MMAc reached 79% with H-Faujasite catalyst at low pressure (a CO pressure of 3 atm). The results were comparable to those of formaldehyde carbonylation catalyzed by solid acid resins in liquid phase at CO pressure of 238 atm [11]. Therefore, it is inherently advantageous to perform the carbonylation of DMM in gas phase. Based on theoretical and kinetic studies, Bell and co-workers suggested that the acid-catalyzed carbonylation of DMM occurred by the Koch-type mechanism [12,13]. For Koch carbonylation reactions, the acid strength of catalysts generally plays a vital role at the catalytic activity. In some cases, only strong acids can effectively catalyze the carbonylation reactions [14,15]. Further studies

* Corresponding author. Tel.: +86 411 84685510; fax: +86 411 84685510.
E-mail address: liuzm@dicp.ac.cn (Z. Liu).

http://dx.doi.org/10.1016/j.apcata.2015.03.010
0926-860X/

by Bell and co-workers showed that the zeolites framework types have a significant influence on the catalytic performance, and high-silica H-Y zeolites are more selective for the carbonylation reaction than other zeolite catalysts because the disproportion of DMM, the side reaction, is suppressed within the relatively large supercages of H-Y zeolites [16]. Thus, according to the present findings, it is of interest to develop new type of catalysts with strong acid sites and large pores for the carbonylation of DMM.

Nafion-H resin, a cross-linked perfluorinated polymeric sulfonic acid resin, appears to be an ideal candidate for the vapor-phase carbonylation of DMM, since the acid strength of Nafion resin is markedly high due to the high electron-withdrawing effect of α-CF_2 moiety attached to the sulfonic acid groups [17]. Also, in contrast with the acid sites located within the channels of zeolites, the acid sites of Nafion resin have no steric constraint of the pore walls. Unfortunately, one major drawback of commercially available resin is the very low surface area, and most active sites are buried in the bulk material. Therefore, they are not accessible for reactants, especially in gas-phase reactions. In order to improve the catalytic efficiency of Nafion resin catalyst, several preparing methods have been adopted to increase the accessibility of acid sites within Nafion resin. For example, Nafion resin has been dispersed onto the high surface area supports, such as highly porous SiO_2 [18], siliceous SBA-15 or MCM-41 materials [19,20] by impregnation method. These supported Nafion catalysts showed improved performance in various reactions, but would suffer from leaching problem in the solvent [21]. An alternative strategy which has attracted much attention is to trap the small Nafion resin particles within highly porous silica matrix by using the sol–gel technique [22]. The obtained composite materials ingeniously have high surface areas and highly available strong acid sites of Nafion resin. The composite have been used as catalysts for various acid-catalyzed reactions, such as acylation [20], alkylation [23], Friedel-Crafts benzylation [24,25], esterification [26], and showed much higher reactivity than the pure Nafion resin. Here, we first reported to employ the composite materials as catalysts for vapor-phase carbonylation of DMM. In this work, Nafion-silica composite catalysts with different Nafion resin loadings were prepared, characterized, and evaluated for the vapor-phase carbonylation of DMM. The same type of results obtained with high-silica acidic zeolites and pure Nafion resin were included for comparison. In addition, the influence of silica sources used for preparation of the composite catalysts on the catalytic activity for DMM carbonylation was discussed as well.

2. Experimental

2.1. Reagents

All the chemicals were obtained commercially and used without any further purification. Nafion NR50 resin, Nafion resin solution (D520, 5.0–5.4 wt% Nafion), tetraethyl orthosilicate (TEOS), colloidal silica and sodium silicate were obtained from Aldrich. High-silica H-Y zeolite (Si/Al = 40) and high-silica H-Beta (Si/Al = 31) zeolite were purchased from Zeolyst and Nankai University catalyst Co., Ltd., respectively.

2.2. Catalysts preparation

In this study, a series of Nafion-silica composite samples with different loadings of Nafion resin were prepared. When using TEOS as the silica source, the composite samples were prepared according to a procedure described elsewhere [22,27]. First, 4 mL deionized water and 1 mL HCl solution (0.1 M) were mixed with 15 g TEOS and stirred for about 1 h (solution A). In another flask, 20 mL NaOH solution (0.1 M) was mixed with 5 g of 5 wt% Nafion solution (solution B). Then, the resulting clear solution A was rapidly added to the solution B under vigorous stirring. Within a few seconds, the gel was formed. After aging at ambient temperature for 4 h, the solid gel was dried for two days in flowing nitrogen at 95 °C, and changed into glass-like solid. The resulting material was gently grounded into smaller particles, treated with 25 wt% nitric acid solution overnight at 75 °C. Finally, the composite catalyst was obtained after drying in a vacuum oven at 95 °C for 24 h. Analogously, the contents of Nafion resin in the samples can be adjusted by varying the amounts of Nafion resin solution. The obtained samples were denoted as TEOS/Nafion-X, where X is referred as the predetermined loadings of Nafion resin.

In addition, other two silica precursors including sodium silicate ("water glass"), and colloidal silica were also used for preparing the Nafion-silica composite in the present work. In the case of using sodium silicate as the silica source, the preparing procedure was modified from a literature method [28]. In a typical procedure, 6.5 mL of HCl solution was added to the 17 g of 2.5 wt% Nafion solution under stirring condition. Then the mixture was rapidly added to the 25 g of a solution of sodium silicate (10 wt% SiO_2) and the gelation immediately occurred. When using colloidal silica as the silica source, 15 g Nafion solution was added to 16.7 g of colloidal silica solution, then, HCl solution (1 M) was added into the mixture to induce the gelation. The drying and re-acidification steps were carried out in the same way as described for the TEOS-based samples. The obtained samples using sodium silicate and colloidal silica as the silica sources were sighed as Na-silicate/Nafion-15 and Col-silica/Nafion-15, respectively.

For comparison, supported Nafion resin catalyst was prepared by impregnating 4.5 g of SiO_2 support into 7 mL of Nafion-H solution containing 10% Nafion-H resin (concentrated from 5 wt% Nafion solution), followed by drying at room temperature for 12 h, then overnight under vacuum condition at 95 °C. Before testing, the sample must be treated with nitric acid solution as described above. The SiO_2-supported Nafion catalyst was sighed as SiO_2/Nafion-15.

2.3. Catalytic test

The tests of DMM carbonylation reaction were carried out in a continuous-flow fixed-bed stainless steel reactor. Typically, an appropriate amount of catalyst was loaded into a reactor tube (8 mm internal diameter). The sample was then heated to 120 °C for an hour under nitrogen atmosphere (30 mL min^{-1}) to remove residual water and then cooled to the reaction temperature. DMM was carried into reactor by carbon monoxide, which was passed through a stainless steel saturator containing liquid DMM isothermally held at 20 °C. The reaction effluent was analyzed by on line gas chromatography (Agilent 7890) equipped with a flame ionization detector. The conversion and selectivity were calculated as follows [10]:

$$\text{DMM conversion} = \left[\frac{1 - 3C_{DMM}}{3C_{DMM} + 2C_{DME} + 2C_{MF} + C_{methanol} + 3C_{MMAc}}\right] \times 100\% \quad (1)$$

$$\text{MMAc selectivity} = \left[\frac{3C_{MMAc}}{2C_{DME} + 2C_{MF} + C_{methanol} + 3C_{MMAc}}\right] \times 100\% \quad (2)$$

where Ci was the molar concentration of compound i in the reaction effluent and n was the number of carbon derived from DMM.

2.4. Characterization of the catalysts

Nitrogen adsorption–desorption isotherms were obtained using a Micromeritics 2020 apparatus. Prior to the measurements, the samples were degassed at 120 °C at high vacuum for 3 h. BET model was used to estimate the surface areas of the samples. The mesopore size was calculated from BJH model using the adsorption branches of isotherms. The pore volumes of samples were calculated by t-plot method.

Scanning electron microscope (SEM) and energy-dispersive X-ray (EDX) microanalyses were obtained using a Hitachi SU8020 apparatus operated at 20 kV. Transmission electron micrographs (TEM) were obtained using a JEM-2100 microscope operated at 200 kV.

IR spectra of adsorbed pyridine (Py-IR) were collected on BRUKERTENSOR 27 FT-IR spectrophotometer. The powder sample was pressed to self-supported wafer, which was then placed into an IR-cell connected to a vacuum system. The sample was outgassed at 150 °C for 1 h under vacuum condition and subsequently exposed to the pyridine vapor for 5 min after cooling down to room temperature. Then, the spectra were recorded at room temperature after evacuating at different temperatures for 30 min.

^{31}P MAS NMR spectrum was recorded on a Bruker AvanceIII 600 spectrometer using a single pulse sequence under the following conditions: π inpulse-width, 2.25 μs; recycle delay, 4 s; sample spinning rate, 12 kHz. Aqueous 85% H_3PO_4 solution was used as external reference for the ^{31}P NMR chemical shift. Prior to the adsorption of trimethylphosphine oxide (TMPO) molecule, Nafion-silica sample was treated in a flask under vacuum at 120 °C for 12 h to remove the adsorbed water molecule. Then, the dehydrated sample was transferred into glovebox and an appropriate amount of TMPO dissolved in CH_2Cl_2 was added to the flask containing the sample. The obtained mixture was stirred overnight to ensure the efficient reaction between acid sites and TMPO molecules. Subsequently, the solvent was removed in flowing N_2 at 40 °C. Finally, the TMPO-loaded sample was transferred into a NMR rotor for NMR test.

The acid site concentrations of samples were determined using aqueous NaCl solutions and titrated by dilute aqueous NaOH. In a typical experiment, 0.5 g of solid was added to 20 mL of NaCl (2 M) solution, and vigorously stirred at room temperature overnight. After removing the solids by centrifugation, the obtained solution was titrated by a drop wise addition of 0.05 M NaOH solution.

The weight loss curves were recorded on SDT Q600 thermal analyzer from ambient temperature to 700 °C at a ramping rate of 10 °C min^{-1} in nitrogen atmosphere to determine the real contents of Nafion resin in the samples (Fig. S1, see supplementary information).

3. Results and discussion

3.1. Catalyst characterization

Compared with the pure Nafion resin, Nafion-silica composite materials prepared by sol–gel method have properties of mesoporous silica matrix with high surface area. Nafion-silica composites presented the advantages of both Nafion resin and mesoporous silica matrix. Here, the detailed information about surface area and porosity of porous materials were obtained by analysis of the nitrogen adsorption/desorption isotherms, which are shown in Fig. S2 (see supplementary information). As can be seen from Fig. S2, all the samples display type-IV isotherms with clear H_1-type adsorption–desorption hysteresis [29], indicating the good development of mesoporosity due to the closely arranged spherical particles [30]. A remarkable difference in the location of the hysteresis loop is observed between samples with different types of silicon sources, i.e. sodium silicate and colloidal silica. The former samples show a hysteresis loop in the P/P_0 rang of 0.6–0.85, whereas the hysteresis loops of the latter samples shift toward higher relative pressures (0.85–0.98), indicating the presence of larger pores. The structural parameters, such as BET surface area, pore volume, and pore diameter, are also summarized in Table 1. It can be seen that the specific surface area of TEOS/Nafion-5 is about 350 m^2 g^{-1}, considerably higher than that of pure Nafion resin (less than 0.02 m^2 g^{-1}) [17]. Here, it should be reminded that both the silica matrix and Nafion resin contribute to the high surface area of Nafion-silica composite material, and the effective surface area of Nafion resin alone in the composite is lower than the apparent value. Harmer and co-workers estimated the effective surface area of Nafion resins to be about 100 m^2 g^{-1} [22]. With the increase of the Nafion resin loadings, the surface area of Nafion-silica composite begins to reduce because too much Nafion resin will disrupt the continuity of the porous silica network or lead to the blockage of the pores. Additionally, though the loadings of Nafion resin are very similar, the surface area of TEOS/Nafion-15 sample is much higher than that of Na-silicate/Nafion-15 and Col-silica/Nafion-15, suggesting that the type of silica sources has a pronounced effect on the microstructure of the synthesized composite samples.

Fig. 1a is an SEM micrograph of the surface of TEOS/Nafion-15 sample. As displayed, the sample appears to be formed by agglomeration of smaller particles. Furthermore, the porosity of the material is confirmed by close examination of the microstructure. Fig. 1b is the TEM micrograph of the TEOS/Nafion-15 sample, again showing the particulate substructure and the porosity indicated by the white areas.

Fig. 2 shows the EDX elemental mapping images of TEOS/Nafion-15 sample. In the images, the bright dots indicate the present of Si, O, F and S and no area enriched entirely in S or F is observed, indicating that Nafion resin is homogeneously distributed within the silica matrix. Indeed, Harmer suggested that Nafion resin and silica can be well intermixed at the nanometer level [22]. It can be expected that the effective surface of Nafion resin in composite material is considerably higher than that of pure Nafion resin, resulting in the great improvement of accessibility of the reactants toward the active sites.

In order to confirm the accessibility of acid sites in the composite catalysts, IR spectra of TEOS/Nafion-15 sample after pyridine adsorption are shown in Fig. 3. It can be seen that three bands at 1545, 1490, and 1445 cm^{-1}, characteristic of bands of Brönsted and Lewis acid, obviously demonstrate the presence of both Brönsted and Lewis acid sites. The band at 1540 cm^{-1} corresponds to the pyridinium ions resulting from the reaction of pyridine with proton sites, and the band at 1445 cm^{-1} indicates the presence of Lewis acid sites. After evacuating at 80 °C for 30 min, the intensity of band at 1445 cm^{-1} decreased significantly, and disappeared after the temperature increased to 150 °C, indicating that the acidity of Lewis acid is rather weak. However, the band at 1544 cm^{-1} remained almost unchanged, even after evacuating at 150 °C These results, therefore, clearly confirm the accessibility of the strong sulfonic acid groups of Nafion resin for the gaseous pyridine molecules and its stability under high temperature condition.

The previous studies have demonstrated that ^{31}P MAS NMR spectroscopy with adsorbed trimethylphosphine oxide (TMPO) is suitable to characterize the acid strength of solid acids [31], because the ^{31}P NMR chemical shift of TMPO molecules adsorbed on Brønsted acid sites can increase with the increase of acid strength [32]. Fig. 4 shows the ^{31}P MAS NMR spectrum of TMPO adsorbed on the TEOS/Nafion-15 sample. As displayed, three peaks at 84, 53 and 36 ppm are observed. The weak peak at 36 ppm is ascribed to crystalline TMPO, and the peak at 53 ppm is attributed to TMPO adsorbed on Lewis acid sites, consistent with the analysis from

Table 1
Textural and chemical properties of the Nafion-silica samples.

Entry	Sample	Nafion-H (wt%)[a]	BET surface ($m^2\ g^{-1}$)[b]	D_{pore} (nm)[c]	V_{pore} ($cm^3\ g^{-1}$)[d]	H^+ capacity (mmol g^{-1})[e]
1	TEOS/Nafion-5	5.7	354	8.4	0.84	0.05
2	TEOS/Nafion-15	15.2	349	6.5	0.73	0.14
3	TEOS/Nafion-30	31.0	264	7.3	0.54	0.24
4	TEOS/Nafion-40	43.7	127	10.2	0.36	0.38
5	TEOS/Nafion-60	60.5	30	13.3	0.09	0.58
6	SiO_2/Nafion-15	18.0	370	5.4	0.61	0.18
7	Na-silicate/Nafion-15	14.5	123	26.0	0.77	0.14
8	Col-silica/Nafion-15	21.8	107	21.3	0.55	0.17

[a] Weight loss of samples in the temperature range of 200–600 °C.
[b] BET surface area.
[c] BJH adsorption average pore diameter.
[d] Single-point pore volume at $P/P0 = 0.975$.
[e] Determined by acid–base titration method.

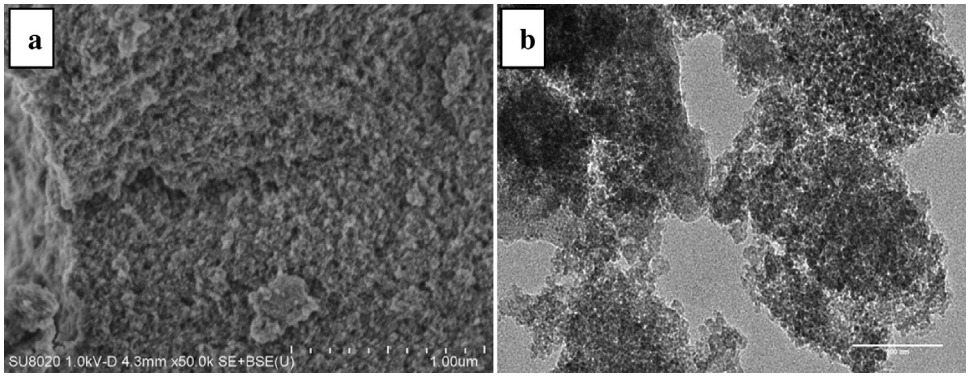

Fig. 1. SEM micrograph (a) and TEM micrograph (b) of the TEOS/Nafion-15 sample.

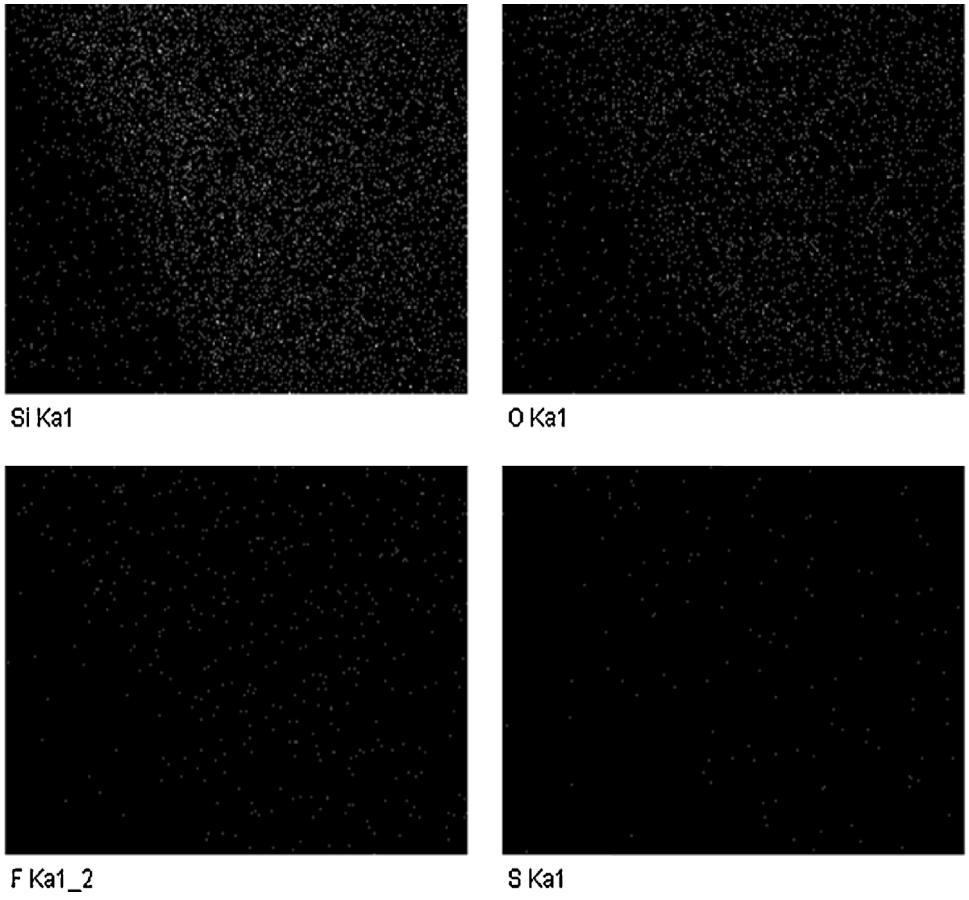

Fig. 2. EDX-mapping images of TEOS/Nafion-15.

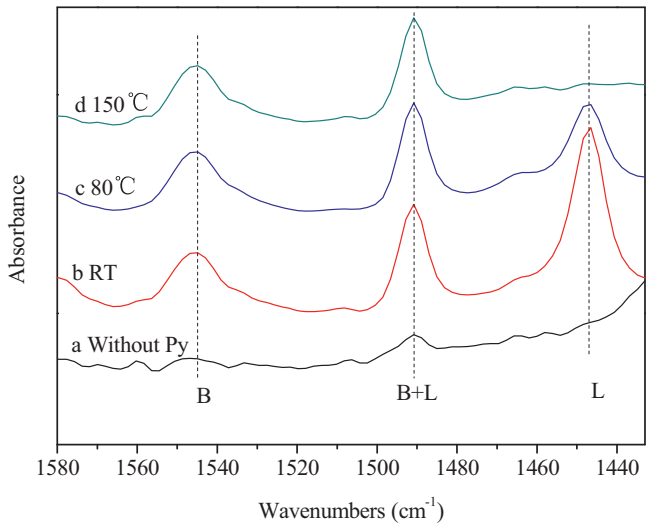

Fig. 3. FT-IR spectra of TEOS/Nafion-15 sample (a) evacuated at 150 °C before pyridine adsorption, after pyridine adsorption and evacuation (b) at room temperature, (c) at 80 °C (d) 150 °C.

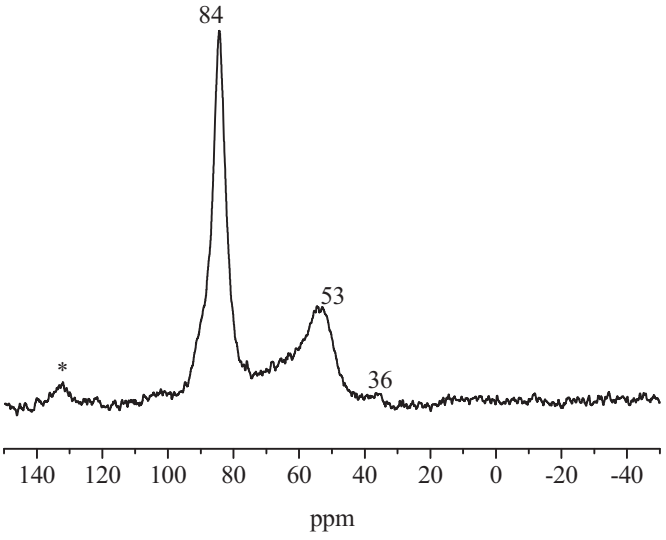

Fig. 4. ^{31}P MAS NMR spectrum of TMPO adsorbed on TEOS/Nafion-15 (asterisk denote spinning sidebands).

Py-FTIR spectra. The strong peak at 84 ppm is associated with TMPO adsorbed on Brönsted acid sites. The value is very close to the threshold value for ^{31}P chemical shift of TMPO adsorbed on solid superacid [32], suggesting that the acid strength of Nafion-silica composite sample is very high.

Additionally, several other parameters related to the acidic properties of Nafion-containing samples are also listed in Table 1. The loadings of Nafion resins on the samples were determined by the weight loss between 200 and 600 °C through thermo decomposition of Nafion resin, and the actual loadings of Nafion resin are well consistent with the acid capacities of samples measured by acid–base titration.

3.2. Catalytic studies

Results of vapor-phase carbonylation of DMM over three different kinds of Nafion catalysts are depicted in Fig. 5. In order to obtain the experimental data that are indicative of intrinsic catalysts, the amounts of Nafion resin in these three tests were equivalent, and

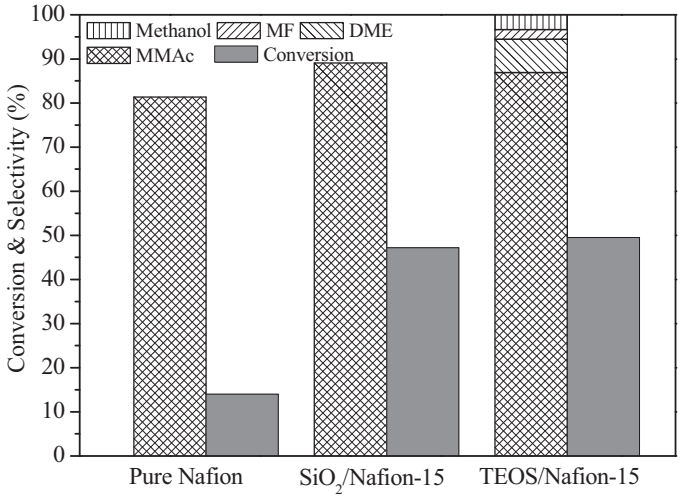

Fig. 5. The catalytic performance DMM carbonylation over different Nafion catalysts at 2 h TOS (reaction conditions: reaction pressure = 30.0 atm, DMM partial pressure = 0.42 atm, CO stream = 85 mL min^{-1}).

the reaction conditions, including reaction temperatures, gas space velocities, reaction pressure and partial pressures of all reactants in all three runs, were nearly the same. In the case of the test with pure Nafion resin, the catalyst was physically mixed with inert silica particles. Clearly, the TEOS/Nafion-15 sample is the most active catalyst among these catalysts, whereas the pure Nafion sample shows the lowest DMM conversion. The results unambiguously demonstrate that catalyst activity of the Nafion catalysts correlates very well with their accessibility of acid sites, i.e., the higher accessibility of acid sites in Nafion resin results in higher catalyst activity. It is also found that Nafion-silica composite sample shows a slightly higher conversion of DMM than silica-supported Nafion catalyst with identical selectivity of MMAc. This difference in catalytic activity may be ascribed to the larger number of surface acid sites on Nafion-silica composite sample compared to the silica-supported Nafion catalyst. It is consistent with the results report by Olah and co-workers [18]. Additionally, as reported in the literature, Nafion-silica composite catalyst also catalyzes the disproportionation of DMM to produce dimethyl ether (DME) and methyl formate (MF) [10], and a small amount of methanol attributed to the decomposition of MF is detected [16].

Fig. 6 shows the effect of Nafion loadings on the catalytic performance of the composite catalysts for the DMM carbonylation reaction. It can be seen that increasing in the loadings of Nafion resin leads to the improvement of catalytic performance, and the conversion of DMM reaches a maximum value, up to 95% when the amount of Nafion resin is 40%. Apparently, the excellent performance of TEOS/Nafion-40 catalyst is attributed to the higher amount of accessible strong acid sites in the composite sample. Though the activity of Nafion-silica catalysts increases with the increase of Nafion contents, the opposite trend occurs when the activity per acid site is considered. The rate of MMAc synthesis is 12.3 mol (mol H$^+$)$^{-1}$ h^{-1} for TEOS/Nafion-5, but only 7.2 mol (mol H$^+$)$^{-1}$ h^{-1} for the TEOS/Nafion-40 sample. When the Nafion resin content increases to 60%, the conversion of DMM decreases some, but the rate of MMAc synthesis has a sharp reduction, which is attributed to the decrease in the number of the accessible acid sites, evidenced by the low specific surface area (only 30 m^2 g^{-1}, seen Table 1).

In Fig. 7, MMAc selectivity and DMM conversion versus TOS for Nafion-silica composite catalysts prepared from different silica precursors have been plotted. It is interesting to note that there is a slight difference in the conversion of DMM between TEOS and

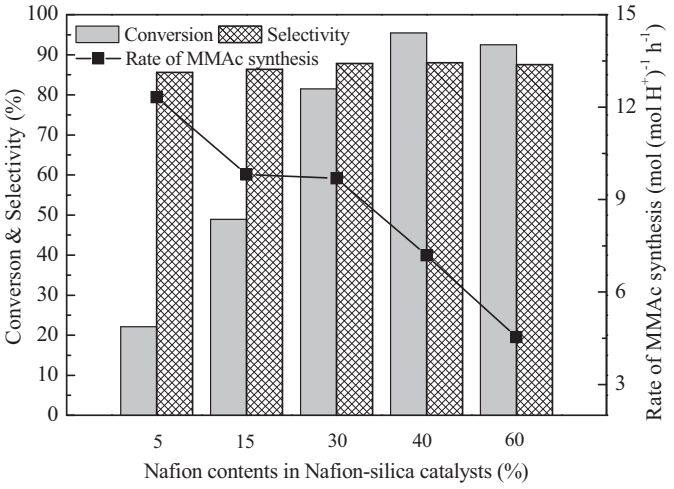

Fig. 6. The effect of loadings of Nafion on the catalytic performance of DMM carbonylation at 2 h TOS (reaction conditions: catalyst weight = 0.4 g, reaction pressure = 30.0 atm, DMM partial pressure = 0.42 atm, CO stream = 85 mL min^{-1}).

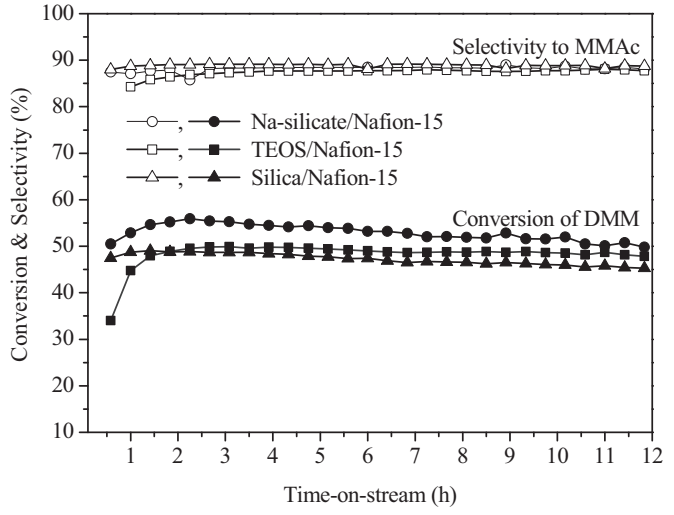

Fig. 7. The carbonylation of DMM over Nafion-silica catalysts derived from different silica sources (reaction conditions: catalyst weight = 0.4 g, reaction pressure = 30.0 atm, DMM partial pressure = 0.42 atm, CO stream = 85 mL min^{-1}).

sodium silicate derived Nafion-silica samples, but the influence on the selectivity of MMAc can be negligible. A plausible explanation for the results is that the silica sources could alter the state of aggregation of Nafion resin within the porous silica matrix, which in turn had a subtle influence on the catalytic reactivity of Nafion-silica catalysts [21]. In addition to the high selectivity, a good catalytic stability is observed on Nafion-silica composite catalyst. For example, the DMM conversion over TEOS/Nafion-15 catalyst decreases from 50% at 2 h on stream to 48% at 12 h on stream.

Fig. 8 provides a comparison of the catalytic performance between the Nafion-silica composite and zeolites catalysts for the vapor-phase carbonylation of DMM. As displayed, Nafion-silica sample shows higher conversion than high-silica H-Y catalyst, but it presents a lower conversion than high-silica H-Beta catalyst. Here, it should be pointed out that the acid density of TEOS/Nafion-15 sample is much lower than that of the acidic zeolites. Thus, the specific rate of the formation of MMAc for TEOS/Nafion-15 is around 9.8 mol (mol H^+)$^{-1}$ h^{-1}, which is higher than those for H-Y and H-Beta zeolite catalysts (2.6 and 2.9 mol mol_{Al}^{-1} h^{-1}, respectively).

The superior catalytic activity of Nafion-silica catalyst is closely related to the strong acid strength of Nafion resin, which was

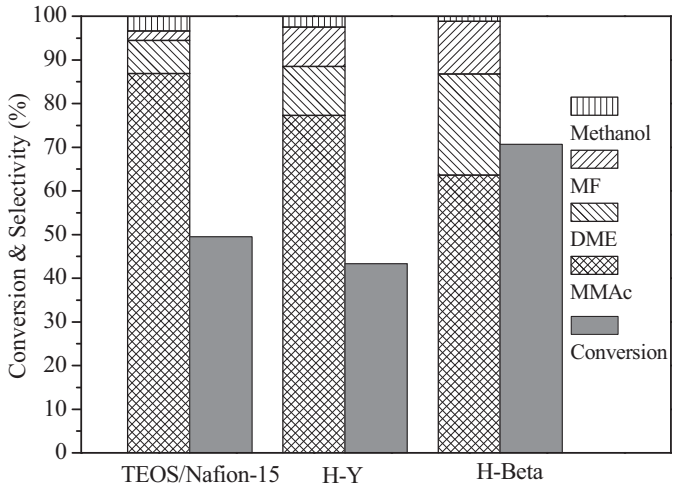

Fig. 8. Carbonylation of DMM over different acid catalysts (reaction conditions: catalyst weight = 0.4 g, reaction pressure = 30.0 atm, DMM partial pressure = 0.42 atm, CO stream = 85 mL min^{-1}).

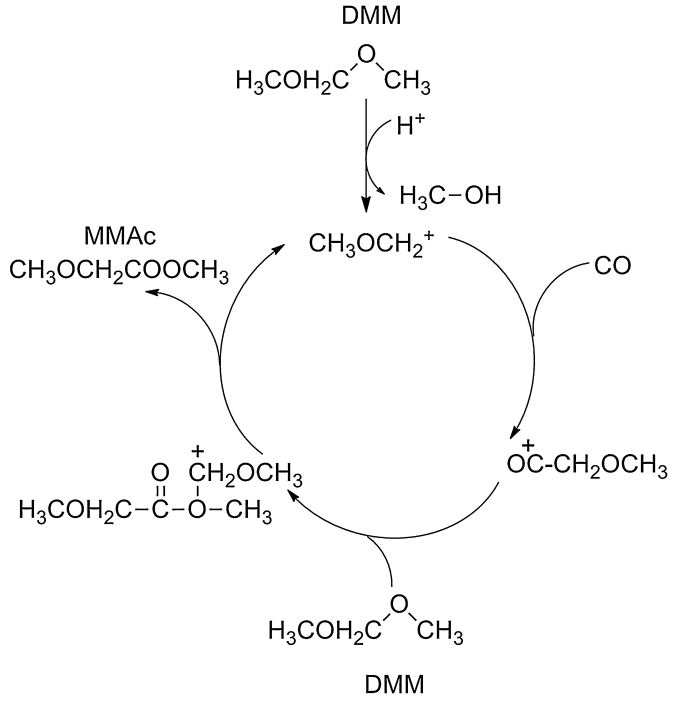

Scheme 1. Proposed mechanism for acid-catalyzed DMM carbonylation.

indicated by the high ^{31}P chemical shift of TMPO adsorbed on the composite catalyst (84 ppm, shown in Fig. 4), while the reported ^{31}P chemical shift of TMPO adsorbed on H-Beta and H-Y zeolites were located at 72 and 65 ppm [33,34], respectively. The observed influence of acid strength on reactivity well reflects the carbocationic nature of acid-catalyzed DMM carbonylation reaction. Based on the previous studies [12,35], a mechanism for acid-catalyzed DMM carbonylation was proposed. As displayed in Scheme 1, the acid-catalyzed DMM carbonylation reaction involves the following elementary steps: DMM are initially protonated by the protons from Brönsted acids to form methoxymethyl species, which are then nucleophilically attacked by CO molecules, forming methoxyacetyl species. The methoxyacetyl species further react with another DMM to produce MMAc and the methoxymethyl species are simultaneously regenerated. Like the typical Koch-type carbonylation reactions (i.e. acid-catalyzed carbonylation

reactions), the reaction between methoxymethyl species and CO affording the methoxyacetyl species has been proved to be the rate-determining step in DMM carbonylation reaction. According to the literatures, the transition state for the carbonyltion step can be described as an association of CO with the methoxymethyl carbocation [10,36]. And, it is well known that increasing the acid strength is beneficial for the stabilization of carbenium ions (e.g. methoxymethyl carbocations), which leads to the decrease in the activation barrier for the carbonylation step [37–39]. Although the confinement effect of zeolite channels has been demonstrated to stabilize the carbenium ions and hence promote the catalytic reactivity of acid-catalyzed carbonylation reactions [13,40–42], the acid strength of Nafion-silica catalyst is considerably higher than that of zeolite catalysts, making the acid strength be the dominant factor governing the reactivity of DMM carbonylation. As a result, Nafion-silica catalyst with higher acid strength presents higher specific catalytic activity for the DMM carbonylation reaction compared to zeolite catalysts. In addition to high activity, it should be noted that Nafion-silica catalyst exhibits the highest selectivity of MMAc among these catalysts, nearly 90%, but the selectivities of MMAc over H-Y and H-Beta zeolites are 80% and 65%, respectively. The difference in the selectivity of MMAc is ascribed to the structures of different types of catalysts. Bell and co-workers have demonstrated that the selectivity of MMAc is significantly influenced by the framework of zeolites, because the steric constraint of small pore channel would promote the disproportion of DMM [16]. As a result, high-silica H-Beta zeolite shows much lower MMAc selectivity than H-Y zeolite which possesses large super cages. In contrast with zeolite catalysts, the pore diameter of Nafion-silica catalyst is in the mesoporous range, much larger than that of zeolite catalysts. Thus, the disproportion of DMM is heavily suppressed, enabling to the highly selective formation of MMAc.

4. Conclusion

We have demonstrated that Nafion-silica composite catalysts prepared by sol–gel method were very efficient and selective for catalyzing DMM carbonylation to produce MMAc in vapor-phase. Comparing with the pure Nafion resin, the excellent activity of Nafion-silica composite materials is apparently attributed to the increased accessibility of active site, ensured by the porous structure and large surface area of the composite material. The mesoporous structure of composite material not only enhances the catalytic efficiency of Nafion resin but also helps suppress the disproportion of DMM, resulting in a higher selectivity of MMAc compared to the microporous acid zeolite catalysts. Furthermore, the catalytic performance of composite catalysts was significantly influenced by the amount of Nafion resin loading. When increasing the loading of Nafion resin to 40%, a nearly complete conversion of DMM (95%) was observed. Additionally, the type of silica sources was found to influence the catalytic reactivity. Sodium silicate derived Nafion-silica sample exhibited a higher conversion than others. The excellent catalytic performance in the DMM carbonylation reaction shows that Nafion-silica composite has significant promise for producing MMAc and its derivatives, such as EG, 2-methoxyethanol and so on.

Appendix A. Supplementary data

Supplementary data associated with this article can be found, in the online version, at http://dx.doi.org/10.1016/j.apcata.2015.03.010.

References

[1] H. Yue, Y. Zhao, X. Ma, J. Gong, Chem. Soc. Rev. 41 (2012) 4218–4244.
[2] http://www.ptq.pemex.com/productosyservicios/eventosdescargas/Documents/Foro%20PEMEX%20Petroqu%C3%ADmica/2012/pci%20oxido%20de%20etileno.pdf
[3] D.J. Loder, US Patent 2,152,852 (1939).
[4] A.T. Larson, US Patent 2,153,064 (1939).
[5] S. Suzuki, US Patent 5,72,780 (1975).
[6] S.Y. Lee, J.C. Kim, J.S. Lee, Y.G. Kim, Ind. Eng. Chem. Res. 32 (1993) 253–259.
[7] S.A.I. Barri, D. Chadwick, Catal. Lett. 141 (2011) 749–753.
[8] Y. Sun, H. Wang, J.H. Shen, H.C. Liu, Z.M. Liu, Catal. Commun. 10 (2009) 678–681.
[9] S.B. Dake, R.V. Chaudhari, J. Chem. Eng. Data 30 (1985) 400–403.
[10] F.E. Celik, T.-J. Kim, A.T. Bell, Angew. Chem. Int. Ed. 48 (2009) 4813–4815.
[11] D.E. Hendriksen, Abstr. Pap. Am. Chem. Soc. 185 (1983) 176–190.
[12] F.E. Celik, T. Kim, A.N. Mlinar, A.T. Bell, J. Catal. 274 (2010) 150–162.
[13] V. Shapovalov, A.T. Bell, J. Phys. Chem. C 114 (2010) 17753–17760.
[14] B.L. Booth, T.A. El-Fekky, J. Chem. Soc. Perkin Trans. 1 (1979) 2441–2446.
[15] S.D. Pirozhkov, A.S. Stepanyan, T.N. Myshenkova, M.B. Ordyan, A.L. Lapidus, Bull. Acad. Sci. USSR Div. Chem. Sci. 31 (1982) 1852–1858.
[16] F.E. Celik, T.-J. Kim, A.T. Bell, J. Catal. 270 (2010) 185–195.
[17] M.A. Harmer, Q. Sun, Appl. Catal. A 221 (2001) 45–62.
[18] B. Török, I. Kiricsi, Á. Molnár, G.A. Olah, J. Catal. 193 (2000) 132–138.
[19] S. Wang, J.A. Guin, Energy Fuels 15 (2001) 666–670.
[20] F. Martínez, G. Morales, A. Martín, R. Van Grieken, Appl. Catal. A 347 (2008) 169–178.
[21] M.A. Harmer, Q. Sun, A.J. Vega, W.E. Farneth, A. Heidekum, W.F. Hoelderich, Green Chem. 2 (2000) 7–14.
[22] M.A. Harmer, W.E. Farneth, Q. Sun, J. Am. Chem. Soc. 118 (1996) 7708–7715.
[23] P. Botella, A. Corma, J. López-Nieto, J. Catal. 185 (1999) 371–377.
[24] Q. Sun, M.A. Harmer, W.E. Farneth, Ind. Eng. Chem. Res. 36 (1997) 5541–5544.
[25] A. Heidekum, M. Harmer, W. Hoelderich, Catal. Lett. 47 (1997) 243–246.
[26] M.J. Climent, A. Corma, S. Iborra, S. Martínez-Silvestre, A. Velty, ChemSusChem 6 (2013) 1224–1234.
[27] M.A. Harmer, Q. Sun, US Patent 5,824,622 (1999).
[28] A. Lassoued, C. Lalo, J. Deson, P. Batamack, J. Fraissard, M. Harmer, D. Corbin, Chem. Phys. Lett. 303 (1999) 368–372.
[29] R. Pierotti, J. Rouquerol, Pure Appl. Chem. 57 (1985) 603–619.
[30] H. Lim, M. Yarmo, N. Huang, P. Khiew, W. Chiu, J. Phys. Sci. 20 (2009) 23–36.
[31] A. Zheng, S.-J. Huang, Q. Wang, H. Zhang, F. Deng, S.-B. Liu, Chin. J. Catal. 34 (2013) 436–491.
[32] A. Zheng, S.-J. Huang, W.-H. Chen, P.-H. Wu, H. Zhang, H.-K. Lee, L.-C.d. Ménorval, F. Deng, S.-B. Liu, J. Phys. Chem. A 112 (2008) 7349–7356.
[33] J. Guan, X. Li, G. Yang, W. Zhang, X. Liu, X. Han, X. Bao, J. Mol. Catal. A: Chem. 310 (2009) 113–120.
[34] S.-J. Huang, Y.-H. Tseng, Y. Mou, S.-B. Liu, S.-H. Huang, C.-P. Lin, J.C. Chan, Solid State Nucl. Magn. Reson. 29 (2006) 272–277.
[35] P. Cheung, A. Bhan, G. Sunley, D. Law, E. Iglesia, J. Catal. 245 (2007) 110–123.
[36] H. Hogeveen, The Reactivity of Carbonium Ions Towards Carbon Monoxide, Elsevier, Amsterdam, 1973.
[37] A.J. Jones, R.T. Carr, S.I. Zones, E. Iglesia, J. Catal. 312 (2014) 58–68.
[38] R.T. Carr, M. Neurock, E. Iglesia, J. Catal. 278 (2011) 78–93.
[39] D.A. Simonetti, R.T. Carr, E. Iglesia, J. Catal. 285 (2012) 19–30.
[40] A. Bhan, A.D. Allian, G.J. Sunley, D.J. Law, E. Iglesia, J. Am. Chem. Soc. 129 (2007) 4919–4924.
[41] A. Bhan, E. Iglesia, Acc. Chem. Res. 41 (2008) 559–567.
[42] H.J. Fang, A.M. Zheng, J. Xu, S.H. Li, Y.Y. Chu, L. Chen, F. Deng, J. Phys. Chem. C 115 (2011) 7429–7439.